Genes Nutr (2007) 2:209–223
DOI 10.1007/s12263-007-0051-4

RESEARCH PAPER

Characterization of intestinal inflammation and identification of related gene expression changes in mdr1a$^{-/-}$ mice

Y. E. M. Dommels · C. A. Butts · S. Zhu · M. Davy · S. Martell · D. Hedderley · M. P. G. Barnett · W. C. McNabb · N. C. Roy

Received: 20 December 2006 / Accepted: 24 January 2007 / Published online: 27 September 2007

Abstract Multidrug resistance targeted mutation (*mdr1a*$^{-/-}$) mice spontaneously develop intestinal inflammation. The aim of this study was to further characterize the intestinal inflammation in *mdr1a*$^{-/-}$ mice. Intestinal samples were collected to measure inflammation and gene expression changes over time. The first signs of inflammation occurred around 16 weeks of age and most *mdr1a*$^{-/-}$ mice developed inflammation between 16 and 27 weeks of age. The total histological injury score was the highest in the colon. The inflammatory lesions were transmural and discontinuous, revealing similarities to human inflammatory bowel diseases (IBD). Genes involved in inflammatory response pathways were up-regulated whereas genes involved in biotransformation and transport were down-regulated in colonic epithelial cell scrapings of inflamed *mdra1*$^{-/-}$ mice at 25 weeks of age compared to non-inflamed FVB mice. These results show overlap to human IBD and strengthen the use of this in vivo model to study human IBD. The anti-inflammatory regenerating islet-derived genes were expressed at a lower level during inflammation initiation in non-inflamed colonic epithelial cell scrapings of *mdr1a*$^{-/-}$ mice at 12 weeks of age. This result suggests that an insufficiently suppressed immune response could be crucial to the initiation and development of intestinal inflammation in *mdr1a*$^{-/-}$ mice.

Keywords Colon · Gene expression · Intestinal Inflammation · Mice

Y. E. M. Dommels · C. A. Butts (✉) · S. Martell · D. Hedderley
Crop & Food Research, Private Bag 11600, Palmerston North 4442, New Zealand
e-mail: buttsc@crop.cri.nz

S. Zhu
The University of Auckland, Private Bag 92019, Auckland 1142, New Zealand

M. Davy
HortResearch, Private Bag 92169, Auckland 1142, New Zealand

M. P. G. Barnett · W. C. McNabb · N. C. Roy
Food, Metabolism & Microbiology, Food & Health Group, AgResearch Limited, Tennent Drive, Private Bag 11008, Palmerston North 4442, New Zealand

Present Address:
Y. E. M. Dommels
Unilever Food & Health Research Institute, PO Box 114, 3130 AC Vlaardingen, The Netherlands

Abbreviations

ABCB	ATP-binding cassette sub-family B
CANX	Calnexin
CYP	Cytochrome P450
IBD	Inflammatory Bowel Diseases
CD	Crohn's Disease
HPRT1	Hypoxanthine phosphoribosyltransferase 1
HIS	Histological injury score
IGFBP7	Insulin-like growth factor binding protein 7
IFN-γ	Interferon gamma
MPO	Myeloperoxidase
MDR	Multidrug resistance
NCF4	Neutrophil cytosolic factor 4
REG3	Regenerating islet-derived 3
RT-PCR	Real time polymerase chain reaction
SNP	Single nucleotide polymorphism
SULT	Sulfotransferase
UC	Ulcerative Colitis

Introduction

Inflammatory Bowel Disease (IBD) refers to two diseases that are characterized by chronic inflammation of the gastrointestinal tract: Crohn's Disease (CD) and Ulcerative Colitis (UC). Both CD and UC share overlap in disease pathology, but also have distinct pathological features. For example, CD can affect any part of the gastrointestinal tract whereas UC is confined to the colon and rectum. The inflammation seen in CD is typically discontinuous, segmental and transmural, involving all layers of the intestinal wall. The lesions in UC are continuous and the inflammation is superficial, only affecting the mucosal layer of the colonic wall [27].

The exact etiology and pathogenesis of IBD is still unclear, but there is strong epidemiological evidence for a genetic contribution to disease susceptibility. Several candidate IBD susceptibility genes have been identified, including a multidrug resistance gene, MDR1 [8, 19]. P-glycoprotein 170, encoded by the human MDR1 (ABCB1) gene and the mouse *mdr1a* (abcb1a) and *mdr1b* (abcb1b) genes, belongs to a family of transmembrane transporters, known as ATP-binding cassette transporters [11]. In the gastrointestinal tract, MDR1 is expressed at the apical surface of intestinal epithelial cells, where it is proposed to actively pump toxins from inside gut cells back into the intestinal lumen, thus decreasing their absorption and bioavailability [3, 11]. The MDR1 gene is located on chromosome 7q, a region for which there is linkage to IBD. Several single nucleotide polymorphisms (SNPs) in MDR1 have been associated with reduced MDR1 activity and have been linked to IBD in some, but not all, populations [4, 12, 25]. Microarray data have also revealed MDR1 as a novel susceptibility gene for IBD. Two independent microarray studies in humans demonstrated a lower expression of MDR1 in colonic biopsies from affected UC and CD patients compared to control subjects [16, 17].

The finding that genetically engineered *mdr1a*$^{-/-}$ mice, with a targeted mutation of the *mdr1a* gene [24], spontaneously develop intestinal inflammation [20] is further evidence that reduced intestinal MDR1 expression or activity may be an important factor in the pathogenesis of IBD. The inflammation seen in *mdr1a*$^{-/-}$ mice was originally classified as similar to UC, but more recent findings suggest a closer resemblance to CD [2]. Observations in *mdr1a*$^{-/-}$ mice that support this suggestion include the location of inflammation (both colon and small intestine), the nature of inflammation (superficial and transmural) and the type of immune response (T-helper cell type 1 response; interferon gamma, IFN-γ) [2, 18].

The mechanistic defect causing inflammation in *mdr1a*$^{-/-}$ mice is unclear, but oral antibiotic treatment both prevented and therapeutically reversed inflammation in *mdr1a*$^{-/-}$ mice, demonstrating the requirement for bacterial flora in the initiation and progression of inflammation in these mice [20]. In addition, infection with *Helicobacter bilis* has been shown to accelerate the development of inflammation, whereas *H. hepaticus* infection delayed the development of inflammation in *mdr1a*$^{-/-}$ mice [18]. We hypothesize that decreased intestinal efflux transport in *mdr1a*$^{-/-}$ mice may lead to a buildup of bacterial products, resulting in an exaggerated or insufficiently suppressed immune response.

The aim of this study was to further characterize the nature, onset and development of inflammation in *mdr1a*$^{-/-}$ mice to better understand the initiation and progression of inflammation in these mice. Sequential histological analysis of intestinal samples was performed over time to verify the time of onset, incidence, location, nature and degree of inflammation. High-density oligonucleotide microarrays were used to identify gene expression changes in colonic epithelial cell scrapings to gain new insight into the immune response associated with initiation and development of inflammation in *mdr1a*$^{-/-}$ mice.

Materials and methods

Animals and diet

A total of 48 male *mdr1a*$^{-/-}$ (FVB.129P2-*PAbcb1a*^{tm1Bor} N7) and 48 male FVB/NTac control mice were purchased from Taconic (Hudson, NY, USA) at 4–5 weeks of age. The mice were initially housed in pairs but, due to fighting, were subsequently housed individually in shoebox-style cages containing untreated wood shavings (Cairns Bins, Palmerston North, NZ) with a plastic tube for environmental enrichment. The animal room was controlled and maintained at a temperature of $\sim$22°C, humidity of $\sim$50% and a 12 h light/dark cycle. All mice were given free access to water and offered an AIN-76A powdered diet prepared in-house (Table 1) ad libitum.

Experimental design

The objective of this experiment was to study the initiation and development of intestinal inflammation and associated changes in gene expression in *mdr1a*$^{-/-}$ mice fed a standard diet as a prerequisite to developing this mouse model for future nutrigenomics studies to explore the effects of changes in nutrition on the development and etiology of IBD. Therefore, for sequential sampling, both *mdr1a*$^{-/-}$ and FVB control mice were randomly divided into eight

Table 1 Composition of the AIN-76A diet

Dietary ingredient	Percentage in the diet (%)
Casein[a]	20
DL-methionine[b]	0.30
Sucrose[c]	50
Dextrin[d]	15
Arbocel, non-nutritive bulk[e]	5
Corn oil[f]	5
Choline bitartrate[g]	0.2
AIN-76A Mineral Mix[h]	3.5
AIN-76A Vitamin Mix[i]	1
Ethoxyquin[j]	0.01

[a] Alacid, Lactic casein 30 mesh, NZMP Ltd, Wellington, New Zealand

[b] Sigma, Sigma-Aldrich Inc, St Louis, MO, USA

[c] Caster sugar, Chelsea, New Zealand Sugar Company Limited, Auckland, New Zealand

[d] Wheaten cornstarch, Golden Harvest, Primary Foods Ltd, Auckland, New Zealand

[e] Arbocell B600, J. Rettenmaier & Sohne GmbH + Co, Rosenberg, Germany

[f] Tradewinds, Davis Trading, Palmerston North, New Zealand

[g] Sigma, Sigma-Aldrich Inc, St Louis, MO, USA

[h] Prepared in-house based on the AIN-76A diet formulation [23]

[i] Prepared in-house based on the AIN-76A diet formulation [23]

[j] Sigma, Sigma-Aldrich Inc, St Louis, MO, USA

sampling groups (9, 12, 16, 22, 25, 27, 29 and 31 weeks of age). All mice were weighed twice a week and carefully monitored for disease symptoms (weight loss, soft faeces, faecal bleeding, posture, gait and inactivity). From around 19 weeks of age, some mortality occurred in the *mdr1a*$^{-/-}$ mice so the last group was sampled at 29 instead of 31 weeks of age. Five days prior to the sampling day those mice allocated for sampling were placed in metabolism cages, offered 3.5–4.0 g/day of the AIN-76A diet and food consumption was measured. Food refusals and spillage were measured to calculate intake. On the last day, mice were fasted overnight (from 3 p.m.) and food was offered 2–4 h prior to sampling in three staggered groups of four mice. All mice were euthanased by CO_2 asphyxiation. The intestine was quickly removed, cut open lengthwise and flushed with 0.9% NaCl to remove any trace of digesta. The intestine was subdivided into duodenum, jejunum, ileum and colon. Two pieces of intact tissue (three for jejunum) at different distal locations per region were collected and stored at room temperature in formalin (10% neutral buffered) for histological analysis. Another intact piece of colon tissue (in between the sections for histology) was snap-frozen in liquid nitrogen and stored at –80°C to measure myeloperoxidase (MPO) activity, a marker of neutrophil infiltration. The epithelial layer of the proximal half of each intestinal region was scraped off, snap-frozen in liquid nitrogen and stored at –80°C for RNA extraction. The experimental procedures for this trial were reviewed and approved by the Crown Research Institute Animal Ethics Committee in Palmerston North, New Zealand according to the Animal Welfare Act 1999.

Histology

The two intact pieces from different areas of each intestinal section (duodenum, jejunum, ileum or colon) were fixed in 10% neutral buffered formalin, embedded in a paraffin block and processed for sectioning. All tissue sections were sliced to obtain sections of 5 μm thickness then stained with haematoxylin and eosin for light microscopic examination. The tissue sections were scored for the following aspects of inflammation: inflammatory lesions (mononuclear cell infiltration, neutrophil infiltration, eosinophil infiltration, plasmocyte infiltration, fibrin exudation and lymphangiectasis), tissue destruction (enterocyte loss, ballooning degeneration, edema and mucosal atrophy) and tissue reparation (hyperplasia, angiogenesis, granulomas and fibrosis). A rating score between 0 (no change from normal tissue) and 3 (lesions involved most areas and all the layers of the intestinal section including mucosa, muscle and omental fat) was given for each aspect of inflammatory lesion, tissue destruction and tissue reparation. The sum of inflammatory lesions (2×), tissue destruction and tissue reparation score was used to represent the total histological injury score (HIS) for each intestinal section. The sum of the inflammatory lesions was multiplied by 2 to give more weight to this value as the inflammation was mainly characterized by inflammatory lesions.

Myeloperoxidase activity

A surrogate marker of inflammation, MPO activity, was also assessed in an intact piece of colon tissue from non-inflamed and inflamed mice using a colourimetric assay as described by Grisham et al. [9]. Colon tissue from 12 and 25 week old FVB and *mdr1a*$^{-/-}$ was used. The tissue was thawed, weighed and homogenized in a buffer (1 ml of buffer per 50 mg of tissue) containing 200 mM sucrose, 20 mM Tris, 1 mM dithiothreitol and a protease inhibitor (complete protease inhibitor cocktail tablets, Roche Diagnostics, New Zealand) (pH 7.4 with HCl). The homogenate was centrifuged at 20,000*g* for 20 min at 4°C and the resulting pellet was dissolved in acetate–HETAB buffer (pH 6.0) and sonicated (2×10 s) to solubilize

MPO. MPO catalyzes the oxidation of 3,3′,5,5′-tetramethylbenzidine by H_2O_2 to yield a blue chromogen with a wavelength maximum at 655 nm. One unit of activity was defined as the amount of enzyme present that produces a change in absorption per minute of 1.0 at 37°C in the final reaction volume containing sodium acetate. Protein content of the colon samples was determined spectrophotometrically using the bicinchoninic acid Protein Assay Kit (Pierce) with bovine serum albumin as a standard.

RNA isolation

Total RNA was isolated from colonic epithelial cell scrapings of both 12 and 25 week old *mdr1a*$^{-/-}$ and FVB mice using TRIzol (Invitrogen, Auckland, NZ) according to the manufacturer's protocol. Total RNA was further purified using the Qiagen RNeasy Mini Kit (Biolab, Palmerston North, NZ). RNA quality was checked with a Bioanalyzer (Agilent Technologies) and the concentration was measured using the Nanodrop (Nanodrop technologies through Biolab). Samples with an OD 260/280 ratio $\geq$2.0 and a Bioanalyzer 28 s/18 s peak ratio $\geq$1.2 were considered acceptable for further analysis. Eight RNA pools were made for gene expression profiling. Each pool consisted of 2 μg purified total RNA extracted from colonic epithelial cell scrapings per animal with two to three animals per pool. There were two pools per sampling group; these included 12 and 25 week old *mdr1a*$^{-/-}$ and FVB mice (*mdr1a*$^{-/-}$12, FVB12, *mdr1a*$^{-/-}$25 and FVB25). A reference pool was made using an equal amount of total purified RNA extracted from colonic epithelial cell scrapings from all individual animals.

cDNA and fluorescent cRNA synthesis

The Low RNA Input Fluorescent Linear Amplification Kit (Agilent Technologies Inc., Palo Alto, CA, USA) was used to synthesize cDNA and fluorescent cRNA. Labelled cRNA was made on the same day for all pools, including the reference pool. Five hundred nanogram of purified total RNA from each pool was reverse transcribed into cDNA using T7 promotor primer and MMLV-RT enzyme according to the manufacturer's protocol. Either cyanine 3-CTP or cyanine 5-CTP (Perkin-Elmer) was added to each pool. A reference design, including a dye-swap, was used. For each sampling group, one of the pools was labelled with Cy5 while the second pool was labelled with Cy3. The reference pool was also labelled with either Cy5 or Cy3, depending on the labelling of the sample pool. Quality and quantity of the cRNA samples was assessed as described above, respectively before continuing with the hybridization.

Microarray hybridization and scanning

The in situ Hybridization Kit-plus (Agilent Technologies) was used to hybridize cRNA samples to Agilent Technologies Mouse G4121A - 22 k 60mer oligo arrays. 0.75 μg Cy3 labelled cRNA and 0.75 μg Cy5 labelled cRNA was hybridized onto the microarray according to the manufacturer's protocol. The cRNA was spiked with control targets to ensure correct hybridization. Hybridization was performed in an Agilent hybridization oven for 17 h at 60°C, rotating at 4 rpm in the dark. After hybridization, slides were washed and dried according to the manufacturer's protocol and scanned using the Axon GenePix 4200A scanner at a photomultiplier tube (PMT) voltage of 450. Spot identification and quantification was performed using GenePix 7.0 software.

Microarray data analysis

Statistical analysis was performed independently by two different researchers using two different software analysis approaches. The first researcher used GeneSpring GX 7.3 expression analysis software (Agilent Technologies). Data were transformed to correct for the dye-swap and a global normalization (Lowess) was applied. A cross gene error model was used to filter out less precise measurements based on control strength. Furthermore, genes with a probability value superior to 0.3 were filtered out prior to analysis. A list of differentially expressed genes was generated for each comparison of interest (*mdr1a*$^{-/-}$12 vs. FVB12 and *mdr1a*$^{-/-}$25 vs. FVB25) via a volcano plot, using the following criteria; probability value inferior to 0.05 and fold-change superior to 2.

The second researcher used Linear models for microarray analysis (Limma) within the Bioconductor framework to independently analyze the experiment. Prior to analysis spots manually flagged as bad were filtered out before applying a within slide global loess normalization (without background correction). For each comparison a list of differentially expressed gene candidates was generated using moderated *t* statistics and false discovery rate control with alpha = 0.05 as a statistical filtering criteria.

Only data that fulfilled the criteria of the Genespring analysis and were in the top 100 list of genes ranked using the moderated *t* statistics and false discovery rate control in Limma were considered as true differentially expressed genes. Only results from the Limma data analysis are shown.

Quantitative real-time polymerase chain reaction

Quantitative real-time polymerase chain reaction (RT-PCR) was performed to confirm changes in mRNA levels identified using microarray analysis. cDNA was synthesized from 1 μg of total RNA from all sample pools and all individual animals using SuperScript II reverse transcriptase (Invitrogen, NZ). SYBR Green quantitative PCR was performed on the real-time rotary analyzer Rotor-Gene 3000 (Corbett Research, Australia), using the Brilliant SYBR Green QPCR Core Reagent Kit (Stratagene, NZ) according to the manufacturer's protocol. One microliter of 100× diluted cDNA and 1.25 μl of a 1:3000 dilution of the SYBR green dye was used in each 25 μl reaction, with a final primer concentration of 400 nM. The following cycles were performed; 1 × 10 min at 95°C, 40 amplification cycles (40 × 30 s 95°C, 60 s 55°C and 60 s 72°C). A dissociation curve was run with each PCR reaction to verify the absence of primer-dimers and genomic DNA amplification. Data were normalized against the housekeeping genes hypoxanthine phosphoribosyltransferase 1 (HPRT1) and/or calnexin (CANX), whose expression levels were unaffected by the different sample conditions (array data not shown).

Primers were designed using the PrimerSelect software (DNASTAR Lasergene). The following primers (GeneWorks Ltd, Auckland, NZ), were used: CYP4B1: lower 5′–ACA GGT GGG TAG AGG CGG AAG C-3′, upper 5′-ACC AGC AGC GAT GTA GGG AGG AG-3′; SULT1C1: lower 5′-TCG CCG GCA CTT CTC TAC ATC A-3′, upper 5′-GAT CCC ACT GCA GGC TCC AAC T-3′; NCF4: lower 5′-CAT GAT GGC CCC TTG TGG AGA-3′, upper 5′-TGC CGG TCT GCG TGC TGA T-3′; REG3A: lower 5′-AGC TGT TTC CTG TTC TCT TCA CCA-3′, upper 5′-TAT ACC CTC CGC ACG CAT TAG TTG-3′; REG3G: lower 5′-AAG GGC CAG AGA AGG AGA AAA TCA-3′, upper 5′-TCA CTG TGG TAC CCT GTC AAG AGC-3′; IGFBP7: lower 5′-CAG CAC CCA GCC CGT TAC TTC-3′, upper 5′-ATC CCA ACC CCT GTC CTC ATC T-3′; H2DMB1: lower 5′-CCT TGG TTC CGG GTT CTG CTC T-3′, upper 5′-TGG GCC TGG GCT TCA TCA TCT-3′; CANX: lower 5′-GCT CCA AAC CAA TAG CAC TGA AAG G-3′, upper 5′-GCA GCG ACC TAT GAT TGA CAA CC-3′; HPRT1: lower 5′-GAG GTC CTT TTC ACC AGC AAG CT-3′, upper 5′-TGA CAC TGG TAA AAC AAT GCA AAC TTT G-3′. A standard curve for all genes including reference genes was generated using serial dilutions of a pooled sample (cDNA from all sample pools) and was included in each run. The mRNA concentrations were determined from the appropriate standard curve. Analysis of each different sample was performed in duplicate per run. Each pooled sample was validated once. The data for the individual animals are the average of two independent runs with duplicate values for each run. To obtain final results, the ratio between the gene of interest and the reference genes (quantified in the same run) was determined and compared between the different conditions (*mdr1a*$^{-/-}$12 vs. FVB12 and *mdr1a*$^{-/-}$25 vs. FVB25).

Statistics

All statistical analyses (body weight, food intake, histology scores, MPO activity and RT-PCR data between individual animals) were performed in GenStat (8th edition, VSN International, Hemel Hempstead, UK, 2005). One-way ANOVA was used to detect significant differences between the groups. Log transformed values were used for the statistical analysis of the HIS, MPO activity and relative mRNA expression (RT-PCR) data. A probability value less than 0.05 was regarded as significant.

Results

Animal body weight and food intake

The average body weight of the 4 to 5 weeks old *mdr1a*$^{-/-}$ and FVB mice was comparable at the beginning of the experiment, respectively 20.9 ± 1.4 and 20.6 ± 1.2 g. During the study, weight loss was observed in *mdr1a*$^{-/-}$ mice, which led to a lower average body weight of the *mdr1a*$^{-/-}$ mice compared to the FVB mice at 12, 22, 25, 27 and 29 weeks of age. This was only significant ($P < 0.05$) at 22 weeks of age (Table 2). Food intake was not significantly different between *mdr1*$^{-/-}$ and FVB mice at any time point of the study (Table 2).

Time of onset and incidence of inflammation

We observed no signs of intestinal inflammation in any of the FVB mice. The first *mdr1a*$^{-/-}$ mouse with histological signs of intestinal inflammation was sampled at 16 weeks of age, but disease symptoms were already observed at an earlier age in this mouse (lower mobility at 13 weeks of age, diarrhea at 14 weeks of age and weight loss at 15 weeks of age). Although the time of onset of inflammation was variable between the *mdr1a*$^{-/-}$ mice, the first visible signs of intestinal inflammation were observed in most mice between 16 and 27 weeks of age. The incidence of intestinal inflammation increased over time and between 25 and 29 weeks of age, all but one of the mice left in the study had developed inflammation by the time they were sampled (Table 3).

Table 2 Body weight, food intake and myeloperoxidase (MPO) activity of *mdr1a*$^{-/-}$ and FVB mice sampled at 9, 12, 16, 22, 25, 27 and 29 weeks of age

Age (weeks)	Body weight (g)[a]		Food intake (g/day)[b]		MPO activity[c]	
	mdr1a$^{-/-}$ mice	FVB mice	*mdr1a*$^{-/-}$ mice	FVB mice	*mdr1a*$^{-/-}$ mice	FVB mice
9	25.5 ± 0.5	25.2 ± 0.5	2.8 ± 0.1	2.6 ± 0.1		
12	25.6 ± 0.7	26.7 ± 0.7	2.6 ± 0.1	2.9 ± 0.1	20.0 ± 13.6	5.4 ± 1.8
16	30.0 ± 1.3	28.3 ± 1.6	2.8 ± 0.1	2.8 ± 0.1		
22	26.5 ± 1.6*	31.6 ± 0.9	2.5 ± 0.2	2.7 ± 0.1		
25	25.5 ± 0.8**	31.4 ± 2.6	2.8 ± 0.3	3.2 ± 0.2	40.6 ± 13.2*	8.3 ± 2.2
27	31.7 ± 1.8	32.8 ± 1.9	3.4 ± 0.2	3.5 ± 0.1		
29	27.0 ± 1.2	31.6 ± 1.3	2.7 ± 0.4	2.9 ± 0.2		

Data are shown as average ± standard error per group of mice sampled

[a] Body weight was measured on the sampling day, 2–4 h after food was returned following fasting

[b] Food intake was measured during the 5 days prior to sampling, when the mice were fed restricted amounts of food (3.5–4 g/day)

[c] MPO activity was measured in intact colon samples of 12 and 25 weeks old *mdr1a*$^{-/-}$ and FVB mice

* $P < 0.05$ *mdr1a*$^{-/-}$ versus FVB mice from the same age (1-way ANOVA)

** Marginal difference between strains ($0.05 < P < 0.10$)

Table 3 Time of onset and incidence of inflammation in *mdr1a*$^{-/-}$ mice

Age in weeks	9	12	16	22	25	27	29
Number of mice sampled							
mdr1a$^{-/-}$ mice (total: 40[a])	6	6	6	8	6	3	5
FVB mice (total: 47[b])	6	5	6	6	6	6	12
Number of mice with inflammation[c]							
mdr1a$^{-/-}$ mice	0	0	1	6	6	3	4
FVB mice	0	0	0	0	0	0	0
Incidence of inflammation (%)							
mdr1a$^{-/-}$ mice	0	0	17	75	100	100	80
FVB mice	0	0	0	0	0	0	0

[a] Eight *mdr1a*$^{-/-}$ mice died during the experiment. Three *mdr1a*$^{-/-}$ mice died at the start of the experiment due to fighting whilst the other five *mdr1a*$^{-/-}$ mice died during the course of the experiment at 19 (1), 20 (2), 21(1) and 26 (1) weeks of age. Three of these mice were sampled and scored for histological signs of inflammation. Their total HIS in the colon varied between 11 and 18, indicating that these mice died due to inflammatory distress

[b] One FVB mouse died at the start of the experiment due to fighting

[c] Mice were regarded as inflamed when their histological injury score in at least 1 of the different intestinal regions was more than 3.5 (all FVB mice had a HIS in either duodenum, jejunum, ileum or colon less then or equal to 3.5)

Location, grade and nature of inflammation

The histological analysis revealed that the average of the total HIS in *mdr1a*$^{-/-}$ mice was the highest in the colon from 16 weeks of age onwards, followed by duodenum, jejunum and ileum. From 22 weeks of age, the average total HIS in the colon was significantly higher in the *mdr1a*$^{-/-}$ mice compared to the FVB mice (Fig. 1). This was also the case in the duodenum and ileum, starting from 22 weeks of age. The significant differences in the average total HIS between *mdr1a*$^{-/-}$ mice and FVB mice were less pronounced in the jejunum, with differences between strains only significant at 25 and 29 weeks of age. It was evident that the average of the total HIS in the colon of the *mdr1a*$^{-/-}$ mice increased up to 25 weeks of age, with no further increase after 27 or 29 weeks of age.

The location of inflammation was variable between the *mdr1a*$^{-/-}$ mice. All of the twenty inflamed *mdr1a*$^{-/-}$ mice had histological signs of inflammation in the colon. Seven of them were only affected in the colon, five of them were affected in all parts of the intestine and the other eight mice showed histological signs of inflammation in both colon

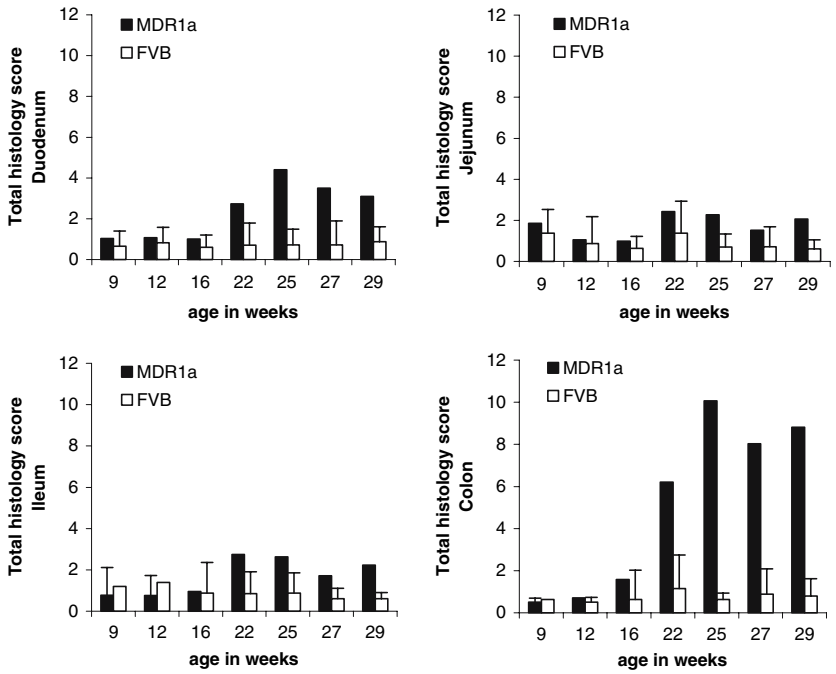

Fig. 1 Total histological injury scores in duodenum, jejunum, ileum and colon of *mdr1a*$^{-/-}$ and FVB mice sampled at 9, 12, 16, 22, 25, 27 and 29 weeks of age. Data are shown as average with LSD bars per sampling group

and different parts of the small intestine (3 colon and ileum, 2 colon and duodenum, 2 colon, jejunum and duodenum and 1 colon, ileum and duodenum).

Intestinal inflammation was mainly characterized by monocyte and neutrophil infiltration and crypt abscess formation, but also enterocyte loss, ballooning degeneration and hyperplasia. The high-grade inflammatory lesions were transmural involving all layers of the intestinal wall and most areas of the tissue section. There was prominent thickening of the mucosal layer and most crypts had disappeared. The remaining crypts showed epithelial cell hyperplasia and a lack of goblet cells (Fig. 2).

Myeloperoxidase activity

The MPO activity was measured as a marker of neutrophil infiltration (inflammation) in intact colon samples of both 12 and 25 weeks old FVB and *mdr1a*$^{-/-}$ mice. The MPO activity was not different between *mdr1a*$^{-/-}$ and FVB mice at 12 weeks of age, but there was a significant increase ($P < 0{\cdot}05$) in MPO activity in colon samples of *mdr1a*$^{-/-}$ mice compared to FVB mice at 25 weeks of age.

Differential gene expression in colonic epithelial cells of non-inflamed mdr1a$^{-/-}$ and non-inflamed FVB control mice at 12 weeks of age

Differential gene expression was assessed in colonic epithelial scrapings of 12 week old *mdr1a*$^{-/-}$ and FVB mice. This sampling group was chosen to identify early changes in gene expression, preceding histological inflammatory changes, because no FVB and *mdr1a*$^{-/-}$ mice from this sampling group showed histological signs of inflammation. Microarray data analysis using two different approaches revealed nine differentially expressed genes between the *mdr1a*$^{-/-}$ mice compared to the FVB mice at 12 weeks of age (Table 4). ATP-binding cassette sub-family B member 1A (ABCB1A or *mdr1a*) and ATP-binding cassette sub-family B member 1B (ABCB1B or *mdr1b*), both involved in drug efflux transport, as well as regenerating islet-derived 3 alpha (REG3A) and regenerating islet-derived 3 gamma (REG3G), both involved in the innate immune response to bacterial colonisation of the gut, were expressed at a lower level in colonic epithelial scrapings of *mdr1a*$^{-/-}$ mice compared to FVB mice.

Furthermore, histocompatibility 2 class II locus Mb1 (H2-DMB1) and major histocompatibility complex class II antigen A beta 1 (H2-HB1), both involved in antigen presentation, ADAM-like decysin 1 (ADAMDEC1), induced during dendritic cell maturation, insulin-like growth factor binding protein 7 (IGFBP7), which can stimulate prostacyclin production, and periostin osteoblast specific factor (POSTN), involved in cell adhesion, were all more highly expressed in colonic epithelial scrapings of *mdr1a*$^{-/-}$ mice compared to FVB mice (Table 4).

Four genes (REG3A, REG3G, IGFBP7 and H2-DMB1), identified by microarray analysis to be differentially expressed at 12 weeks of age, were randomly chosen for validation using RT-PCR. The differential expression of all of these genes was confirmed using pooled RNA samples

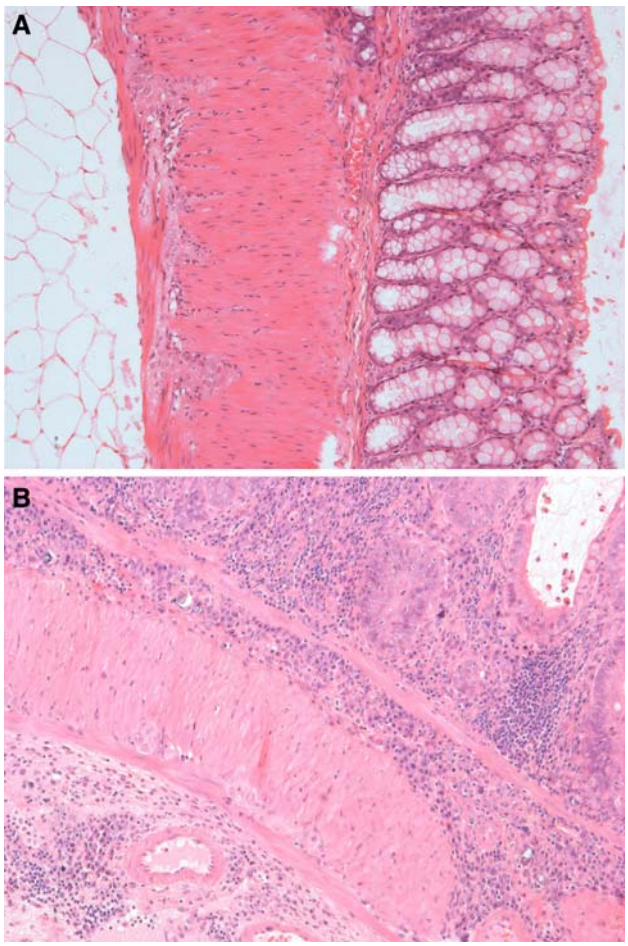

Fig. 2 H&E-stained colon sections of an FVB and an *mdr1a*$^{-/-}$ mouse at 25 weeks of age. **a** Colon section (×100) from an FVB mouse with a normal, non-inflamed appearance. **b** Colon section (×100) from an *mdr1a*$^{-/-}$ mouse with a severely inflamed colon. Lesions involve most of the colon section with monocyte and neutrophil infiltration, crypt abscesses and loss of crypt cells

and RNA samples from individual animals (Table 6; Fig. 3a–d). However the difference in relative mRNA expression of IGFBP7 was not statistically significant ($P = 0.129$) between the individual *mdr1a*$^{-/-}$ and FVB mice.

Differential gene expression in colonic epithelial cells of inflamed mdr1a$^{-/-}$ and non-inflamed FVB control mice at 25 weeks of age

Differential gene expression was also assessed in colonic epithelial scrapings of 25 week old inflamed *mdr1a*$^{-/-}$ and non-inflamed FVB control mice (Table 5). This sampling group was chosen to identify genes with an altered expression during inflammation in *mdr1a*$^{-/-}$ mice. Microarray data analysis using Genespring and Limma software revealed a clear dysregulation of genes involved in xenobiotic metabolism and transport and the immune response. Genes involved in xenobiotic metabolism such as cytochrome P450 (CYP4B1, CYP2C9, CYP2C18), sulfotransferase (SULT1C1), flavin containing monooxygenase (FMO5), carboxylesterase (CES1), aldo-keto reductase (AKR1C4, AKR1C3) and the transporters *mdr1a, mdr1b,* solute carrier family 10, member 2 (SLC10A2) and solute carrier family 13, member 1 (SLC13A1) were expressed at a lower level in colonic epithelial scrapings of inflamed *mdr1a*$^{-/-}$ mice compared to non-inflamed FVB control mice. Inflammatory genes, such as genes involved in the complement system (C1QA, C2, C3), activation of B lymphocytes (SLAM family member 8; SLAMF8), phagocytosis/oxidative burst (neutrophil cytosolic factor 4; NCF4), cell adhesion (integrin beta 7; ITGB7, carcinoembryonic antigen-related cell adhesion molecule 10; CEACAM10) eicosanoid production (IGFBP7) and several chemokines and cytokines (lymphotoxin beta; LTB, chemokine (C-X-C motif) ligand 9 and 10; CXCL9-10, chemokine (C-C motif) ligand 8; CCL8, tumor necrosis factor, alpha-induced protein 2; TNFAIP2 and transcriptional regulators of genes involved in the immune system (nuclear factor of kappa light polypeptide gene enhancer in B-cells inhibitor, zeta; NFKBIZ and CCAAT/enhancer binding protein delta; CEBPD) were more highly expressed in colonic epithelial scrapings of inflamed *mdr1a*$^{-/-}$ mice compared to non-inflamed FVB control mice. Furthermore, several genes involved in cell proliferation and cell death (cyclin D2; CCND2, RNA binding motif, single stranded interacting protein 1; RBMS1, epithelial membrane protein 3; EMP3, follistatin-like 1; FSTL1, hexokinase 2; HK2, S100 calcium binding protein A4; S100A4, serpin peptidase inhibitor, clade A, member 3G; SERPINA3G) as well as energy metabolism (HK2, SLC16A3, ATPase H^+/K^+ transporting, non-gastric, alpha polypeptide; ATP12A) were also more highly expressed in colonic epithelial scrapings of inflamed *mdr1a*$^{-/-}$ mice compared to non-inflamed FVB control mice.

Three genes (CYP4B1, SULT1C1 and NCF4), identified by microarray analysis as differentially expressing at 25 weeks of age, were randomly chosen for validation using real-time RT-PCR. The differential expression of all of these genes was confirmed using pooled RNA samples and RNA samples from individual animals (Table 6; Fig. 3e–g).

Discussion

The precise mechanistic defect causing intestinal inflammation in *mdr1a*$^{-/-}$ mice is unclear but decreased intestinal efflux transport due to defective *mdr1a* expression may lead to a build-up of bacterial products which can result in

Table 4 Differential gene expression in colonic epithelial cells of 12 week old non-inflamed *mdr1a*$^{-/-}$ mice and 12 week old non-inflamed FVB mice

Gene name	Symbol	Refs eq. number	Fold-change *mdr1a*$^{-/-}$ vs. FVB	*P* value	Adjusted *P* value	*T* test ranking
Genes with lower expression in mdr1a$^{-/-}$ mice						
Regenerating islet-derived 3 alpha	REG3A	NM_011036	−7.5	0.02643	0.99997	94th
Regenerating islet-derived 3 gamma	REG3G	NM_011260	−6.4	0.00657	0.99997	27th
ATP-binding cassette, sub-family B, member 1A	ABCB1A	NM_011076	−4.0	0.0001	0.43843	5th
ATP-binding cassette, sub-family B, member 1B	ABCB1B	NM_011075	−3.5	0.00007	0.43843	3rd
Genes with higher expression in mdr1a$^{-/-}$ mice						
Histocompatibility 2, class II, locus Mb1	H2-DMB1	NM_010387	+4.6	0.00004	0.41487	2nd
ADAM-like, decysin 1	ADAMDEC1	NM_021475	+4.2	0.00254	0.99997	16th
Major histocompatibility complex, class II, antigen A, beta 1	H2-HB1	NM_207105	+3.2	0.00257	0.99997	17th
Insulin-like growth factor binding protein 7	IGFBP7	NM_008048	+2.6	0.00009	0.43843	4th
Periostin, osteoblast specific factor	POSTN	NM_015784	+1.8	0.00779	0.99997	34th

an exaggerated or insufficiently suppressed immune response. This study provides new insight into gene expression changes associated with initiation and development of inflammation in *mdr1a*$^{-/-}$ mice. The anti-inflammatory regeneration islet derived 3A (REG3A) and 3G (REG3G), both involved in the innate immune response to bacterial colonisation of the intestine [14], were expressed at a lower level during inflammation initiation in colonic epithelial cell scrapings of 12 week old non-inflamed *mdr1a*$^{-/-}$ mice compared to FVB control mice. This was accompanied by a higher expression of genes involved in antigen uptake, presentation and cell adhesion such as H2-DMB1, H2-HB1, ADAMDEC1 and POSTN. Dysregulated genes that have an altered expression during colonic inflammation in *mdr1a*$^{-/-}$ mice were also identified in this study. This includes several genes involved in both the innate and adaptive immune system that were expressed at a higher level whereas genes involved in xenobiotic metabolism were expressed at a lower level in colonic epithelial cell scrapings of 25 week old inflamed *mdr1a*$^{-/-}$ mice compared to non-inflamed FVB control mice.

Our study confirms the results of a previous study [2] that the colon was the most highly inflamed area of the whole intestine in *mdr1a*$^{-/-}$ mice. The inflammation in *mdr1a*$^{-/-}$ mice was transmural and discontinuous, affecting different layers of the intestinal wall and occurring in different parts of the intestinal tract, revealing similarities to human CD. The time of onset of inflammation was variable; our study: from 16 to 27 weeks of age versus Banner's study: 6 to 11 weeks of age. The cause of accelerated development of inflammation in *mdr1a*$^{-/-}$ mice in Banner's study compared to our study is unknown. Banner et al. [2] failed to detect any known pathogen as the causing factor. Stressors related to animal husbandry practices which are not identical between these studies have been shown to affect the development of inflammatory diseases [13].

The nature of the inflammatory response in CD is thought to be dominated by a T-helper cell type 1 response [21], with stimulation of production of cytokines such as interferon-gamma (IFN-γ) which activate macrophages and induce killer mechanisms, including cytotoxic T cells [5]. We measured plasma cytokine levels using Bead Array and observed an increase in IFN-γ in plasma of 25 week old inflamed *mdr1a*$^{-/-}$ mice compared to FVB control mice. This result was however not significant due to the high variation between the animals (data not shown). It does, however, provide further support for a similarity to human CD as significant increases in both colonic IFN-γ and mRNA for IFN-γ were found in *mdr1a*$^{-/-}$ mice compared to *mdr1a*$^{+/+}$ mice in studies of both Banner et al. [2] and Maggio-Price et al. [18].

The inflammatory lesions in *mdr1a*$^{-/-}$ mice were dominated by agranular monocytes and granular neutrophils, both capable of phagocytosis of toxins and bacteria and inducing an oxidative burst [5]. Neutrophils have been implicated as possible mediators of mucosal injury and indicate an acute inflammatory response [9]. Our visual observations confirm acute inflammation in *mdr1a*$^{-/-}$ mice. When mice developed disease symptoms (diarrhea and weight loss) they needed to be sampled promptly, as it was unlikely they would have survived the inflammatory distress. The total HIS in colon did not increase over time after 25 weeks of age, which also represents the incidence of acute inflammation rather than a chronic accumulation of inflammation over time. The MPO activity, measured as an independent marker of neutrophil infiltration, was also increased in intact colon samples of 25 week old inflamed *mdr1a*$^{-/-}$ mice compared to non-inflamed FVB control mice. Furthermore the gene neutrophil cytosolic factor 4

Table 5 Differential gene expression in colonic epithelial cells of 25 week old inflamed *mdr1a*$^{-/-}$ mice and 25 week old non-inflamed FVB mice

Gene name	Symbol	Refs eq. number	Fold-change *mdr1a*$^{-/-}$ vs. FVB	*P* value	Adjusted *P* value	*T* test ranking
Genes with lower expression in mdr1a$^{-/-}$ mice						
ATP-binding cassette, sub-family B, member 1A	ABCB1A	NM_011076	–5.8	0.00001	0.00558	28th
Cytochrome P450, family 4, subfamily B, polypeptide 1	CYP4B1	NM_007823	–7.0	0.00002	0.01184	54th
Cytochrome P450, family 2, subfamily C, polypeptide 9	CYP2C9	NM_028089	–6.9	0.00008	0.01929	95th
Sulfotransferase family, cytosolic, 1C, member	SULT1C1	NM_026935	–5.9	0.000008	0.00561	34th
Hexokinase domain containing 1	HKDC1	NM_145419	–5.9	0.000005	0.00480	21th
Phospholipid scramblase 2	PLSCR2	NM_008880	–4.9	0.0000002	0.00333	1st
Aldo-keto reductase family 1, member C4	AKR1C4	NM_0010137	–5.0	0.00007	0.01821	82th
Solute carrier family 10, member 2	SLC10A2	NM_011388	–4.4	0.00003	0.01341	58th
Flavin containing monooxygenase 5	FMO5	NM_010232	–4.4	0.000008	0.00561	32th
Chromogranin B	CHGB	NM_007694	–4.3	0.000002	0.00448	5th
Chromogranin A	CHGA	NM_007693	–4.3	0.000005	0.00480	22nd
ATP-binding cassette, sub-family B, member 1B	ABCB1B	NM_011075	–3.6	0.00003	0.01159	53th
Bone morphogenic protein 3	BMP3	NM_173404	–3.4	0.00002	0.00869	39th
Carboxylesterase 1	CES1	NM_053200	–3.3	0.00004	0.01427	64th
Cytochrome P450, family 2, subfamily C, polypeptide 18	CYP2C18	NM_010003	–3.5	0.00008	0.01929	94th
Endothelin 2	EDN2	NM_007902	–3.3	0.00004	0.01370	61st
Solute carrier family 13, member 1	SLC13A1	NM_019481	–3.2	0.00005	0.01686	72nd
Hydroxyprostaglandin dehydrogenase 15-(NAD)	HPGD	NM_008278	–3.5	0.000002	0.00448	9th
Aldo-keto reductase family 1, member C3,	AKR1C3	NM_134066	–2.8	0.00006	0.01819	79th
Major histocompatibility complex, class I, F	HLA-F	NM_008199	–3.2	0.00009	0.02096	100th
Hydroxysteroid dehydrogenase-3, delta <5> –3-beta	HSD3B3	NM_001012306	–2.9	0.00004	0.01427	68th
Hypothetical protein MGC17301	MGC17301	NM_027853	–2.9	0.00004	0.01349	59th
Family with sequence similarity 14, member A	FAM14A	NM_145449	–2.8	0.00002	0.00869	40th
Histocompatibility 2, T region locus 3	H2-T3	NM_008208	–2.5	0.000002	0.00448	4th
Dihydropyrimidine dehydrogenase	DPYD	NM_170778	–2.0	0.00003	0.01185	56th
Riboflavin kinase	RFK	NM_019437	–2.2	0.00001	0.00864	38th
Adenosine kinase	ADK	NM_134079	–2.1	0.00005	0.01686	71th
Genes with higher expression in mdr1a$^{-/-}$ mice						
Gelsolin	GSN	NM_146120	+2.1	0.00003	0.01129	48th
Integrin, beta 7	ITGB7	NM_013566	+2.0	0.00004	0.01370	63th
GTP cyclohydrolase 1	GCH1	NM_008102	+2.1	0.00006	0.01819	77th
RIKEN cDNA 2210407C18 gene	2210407C18Rik	NM_144544	+2.4	0.000003	0.00448	14th
Nuclear factor of kappa light polypeptide gene enhancer in B-cells inhibitor, zeta	NFKBIZ	NM_030612	+2.4	0.000008	0.00561	33nd
Complement component 2	C2	NM_013484	+2.5	0.00007	0.01925	86th
Coactosin-like 1	COTL1	NM_028071	+2.7	0.000003	0.00448	15th
Hypothetical protein FLJ21511	FLJ21511	NM_145560	+2.6	0.00007	0.01919	84th
Cyclin D2	CCND2	NM_009829	+2.5	0.00004	0.01355	60th

Table 5 continued

Gene name	Symbol	Refs eq. number	Fold-change *mdr1a*$^{-/-}$ vs. FVB	*P* value	Adjusted *P* value	*T* test ranking
Glia maturation factor, gamma	GMFG	NM_022024	+2.6	0.00006	0.01737	74th
Leucine aminopeptidase 3	LAP3	NM_024434	+2.9	0.000005	0.00514	23rd
Lymphotoxin beta	LTB	NM_008518	+2.8	0.00005	0.01485	69th
CEA-related cell adhesion molecule 10	CEACAM10	NM_007675	+2.9	0.00004	0.01427	66th
Membrane-spanning 4-domains, subfamily A, member 7	MS4A7	NM_027836	+2.5	0.00006	0.01819	78th
RNA binding motif, single stranded interacting protein 1	RBMS1	NM_020296	+2.9	0.000004	0.00480	18th
Epithelial membrane protein 3	EMP3	NM_010129	+2.9	0.00003	0.01129	50th
Dickkopf homolog 3	DKK3	NM_015814	+2.7	0.00003	0.01129	51st
Milk fat globule-EGF factor 8 protein	MFGE8	NM_008594	+3.3	0.00006	0.01819	75th
Myosin, light polypeptide 7. regulatory	MYL7	NM_022879	+3.4	0.00002	0.00869	42nd
SLAM family member 8	SLAMF8	NM_029084	+2.8	0.00002	0.01071	47th
Follistatin-like 1	FSTL1	NM_008047	+2.7	0.00009	0.01977	98th
Calponin 1, basic, smooth muscle	CNN1	NM_009922	+3.3	0.00008	0.01929	90th
Hexokinase 2	HK2	NM_013820	+4.0	0.000007	0.00549	27th
Annexin A8	ANXA8	NM_013473	+4.5	0.000003	0.00448	13th
Zinc finger CCCH-type containing 12A	ZC3H12A	NM_153159	+3.6	0.000006	0.00520	25th
CCAAT/enhancer binding protein (C/EBP), delta	CEBPD	NM_007679	+4.0	0.000001	0.00448	3rd
Small proline-rich protein 1A	SPRR1A	NM_009264	+3.7	0.000003	0.00448	10th
Solute carrier family 16, member 3	SLC16A3	NM_030696	+3.8	0.00002	0.00869	41st
Collagen, type I, alpha 2	COL1A2	NM_007743	+3.7	0.00003	0.01129	49th
S100 calcium binding protein A4	S100A4	NM_011311	+4.0	0.000003	0.00448	8th
Insulin-like growth factor binding protein 7	IGFBP7	NM_008048	+4.0	0.000002	0.00448	7th
HtrA serine peptidase 1	HTRA1	NM_019564	+3.6	0.000003	0.00448	16th
Serine (or cysteine) peptidase inhibitor, clade A, member 3G	SERPINA3G	NM_009251	+4.0	0.00008	0.01929	89th
Chemokine (C-X-C motif) ligand 9	CXCL9	NM_008599	+4.2	0.00007	0.01925	85th
Tumor necrosis factor, alpha-induced protein 2	TNFAIP2	NM_009396	+4.2	0.00008	0.01929	96th
Membrane-spanning 4-domains, subfamily A, member 6B	MS4A6B	NM_027209	+4.5	0.000002	0.00448	6th
Neutrophil cytosolic factor 4	NCF4	NM_008677	+4.7	0.00002	0.01071	45th
Serpin peptidase inhibitor, clade H, member 1	SERPINH1	NM_009825	+5.1	0.00003	0.01185	55th
Enolase 3	ENO3	NM_007933	+5.9	0.000009	0.00570	36th
Decorin	DCN	NM_007833	+6.6	0.00008	0.01929	93rd
Chemokine (C-X-C motif) ligand 10	CXCL10	NM_021274	+7.6	0.00007	0.01821	83rd
Chemokine (C-C motif) ligand 8	CCL8	NM_021443	+8.4	0.00009	0.02046	99th
Complement component 1, q subcomponent, alpha polypeptide	C1QA	NM_007572	+12.1	0.000008	0.00561	30th
ATPase, H^+/K^+ transporting, nongastric, alpha polypeptide	ATP12A	NM_138652	+10.6	0.0000005	0.00448	2nd
Complement component 3	C3	NM_009778	+15.0	0.000008	0.00570	35th

(NCF4) (alias p40-phox) was expressed at a higher level in colonic epithelial cell scrapings of 25 week old inflamed *mdr1a*$^{-/-}$ mice. NCF4 is a component of the NADPH-oxidase multiple component enzyme system [15], responsible for the oxidative burst in which electrons are transported from NADPH to molecular oxygen, generating

Table 6 Validation of microarray data using real-time RT-PCR

Gene symbol	Fold-change *mdr1a*$^{-/-}$ vs. FVB microarray		Fold-change *mdr1a*$^{-/-}$ vs. FVB RT-PCR HPRT[a]		Fold-change *mdr1a*$^{-/-}$ vs. FVB RT-PCR CANX[a]	
	12 weeks	25 weeks	12 weeks	25 weeks	12 weeks	25 weeks
Randomly chosen differentially expressed genes at 12 weeks of age						
REG3A	–7.5	–25.3[b]	–13.0	–57.2	–8.6	–31.6
REG3G	–6.4	–6.3[b]	–8.6	–6.2	–7.7	–6.0
H2-DMB1	+4.6	+2.1[c]	+9.1	+3.8	+9.1	+3.6
IGFBP7	+2.6	+4.0	+4.1	+9.0	+5.5	+13.9
Randomly chosen differentially expressed genes at 25 weeks of age						
NCF4	+1.6[c]	+4.7	+1.3	+5.8	+1.3	+5.0
CYP4B1	–1.1[c]	–7.0	–1.1	–7.5	–1.2	–6.8
SULT1C1	–1.1[c]	–5.9	–1.4	–10.6	–1.3	–8.4

[a] Two different house-keeping genes were chosen for normalisation of the data; hypoxanthine phosphoribosyltransferase 1 (HPRT1) and calnexin (CANX)

[b] Microarray result was not in the top 100 list of genes ranked by P value using the moderated t-statistics and FDR in Limma, but fulfilled the criteria of the Genespring analysis (FC $\geq$ 2, P value < 0.05)

[c] Microarray result was not statistically significantly different using either GeneSpring or Limma

reactive oxygen intermediates crucial for host defense. This result also agreed with the increased neutrophil infiltration in colonic epithelial cells of inflamed *mdr1a*$^{-/-}$ mice.

REG3A and REG3G were expressed at a lower level in colonic epithelial cell scrapings of 12 week old non-inflamed *mdr1a*$^{-/-}$ mice compared to FVB control mice. Regeneration islet derived (REG) genes, the murine orthologues of human pancreatitis-associated proteins (PAP), are part of the innate immune response and have been shown to be induced after colonisation of germ-free SCID mice with commensal bacteria [14]. Recently it was shown that PAP1 has functional similarities to the cytokine interleukin 10 (IL-10) and can inhibit the inflammatory response by blocking NFκB activation [7]. Down-regulation of the anti-inflammatory REG (PAP) genes in non-inflamed *mdr1a*$^{-/-}$ mice of 12 weeks of age suggests that an insufficiently suppressed immune response could be crucial to the initiation and development of intestinal inflammation in *mdr1a*$^{-/-}$ mice. Down-regulation of the anti-inflammatory REG (PAP) genes could lead to more active NFκB and more transcriptional activation of pro-inflammatory genes such as adhesion molecules [26] and MHC class II genes [10]. The lower expression of the REG (PAP) genes in colonic epithelial cell scrapings of 12 week old non-inflamed *mdr1a*$^{-/-}$ mice compared to non-inflamed FVB control mice was accompanied by a higher expression of a cell adhesion molecule (POSTN) and two MHC class II genes (H2-DMB1 and H2-HB1), suggesting more active NFκB in *mdr1a*$^{-/-}$ mice.

Other inflammatory genes that are more highly expressed in 25 week old inflamed *mdr1a*$^{-/-}$ mice compared to FVB control mice include those involved in the complement system (C1QA, C2, C3), activation of B lymphocytes (SLAMF8), cell adhesion (ITGB7, CEACAM10), eicosanoid production (IGFBP7) and several chemo- and cytokines (LTB, CXCL9, TNFAIP2, CXCL10, CCL8). Two transcriptional regulators of genes involved in the immune system NFKBIZ and CEBPD were also expressed at a higher level in inflamed *mdr1a*$^{-/-}$ mice. Several similar genes such as complement component genes (C2, CR2, C4a), a neutrophil chemotaxin (NCF1), an integrin (ITGB2) and the cytokines LTB [6], CXCL1, CXCL3, CXCL8 and CCL20 [22] were also found to be more highly expressed in colonic and mucosal biopsies of patients with IBD.

Using DNA microarrays, a cluster of strongly down-regulated genes has been identified in the colon of patients with IBD [16]. This cluster of genes was composed of cellular detoxification and defense genes, such as cytochrome P450 enzymes, a carboxylesterase (CES2), glutathione S-transferases, sulfotransferases and ABC transporters. Our data are in good agreement with these human studies as several cytochrome P450s (CYP4B1, CYP2C9, CYP2C18), a sulfotransferase (SULT1C1), a carboxylesterase (CES1) and the ABC transporter ABCB1B (*mdr1b*) were strongly down-regulated in the colon of inflamed *mdr1a*$^{-/-}$ mice, as were several other xenobiotic metabolism genes such as aldo-keto reductases (AKR1C4, AKR1C3) and a flavin containing monooxygenase (FMO5). A decrease in the expression of detoxification enzymes and transporters is probably a secondary effect. Inflammation and infection have long been

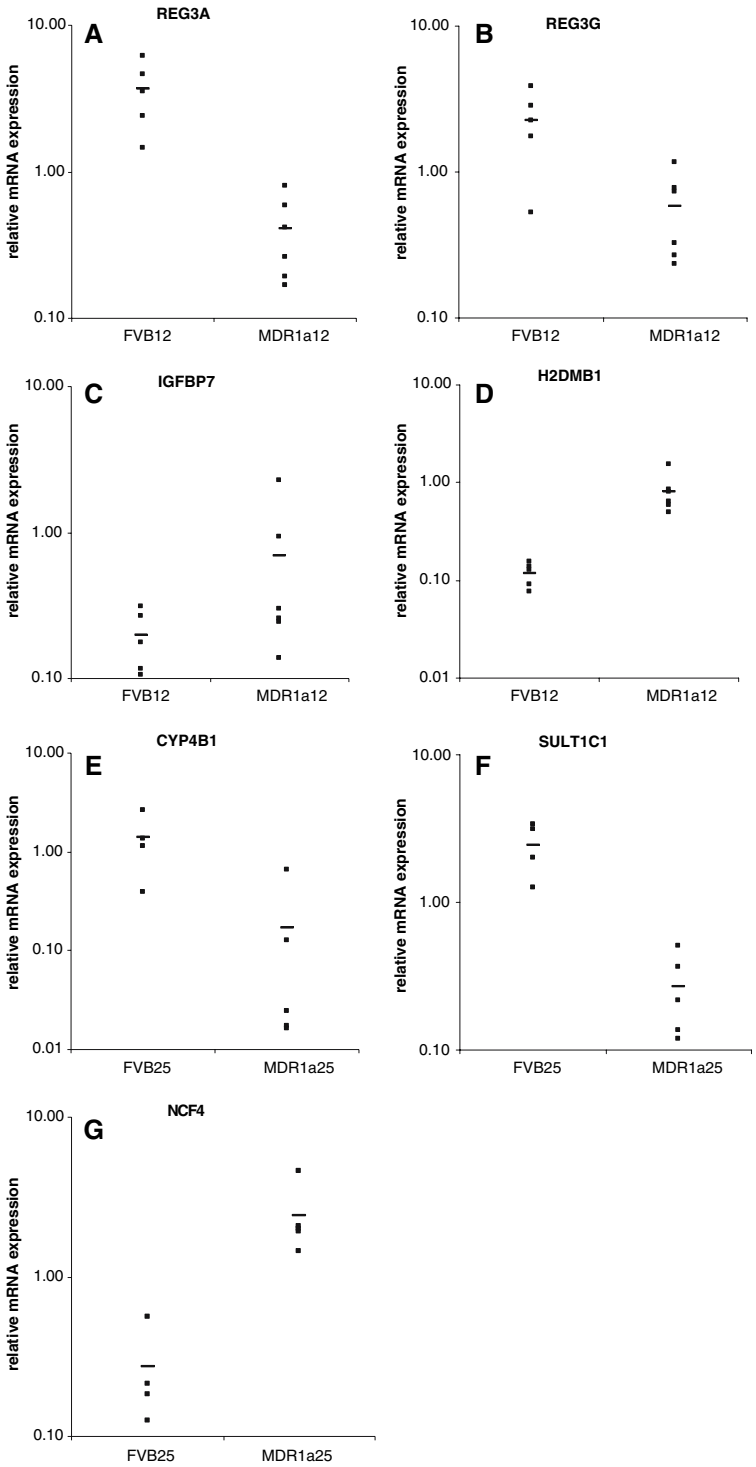

Fig. 3 Differential gene expression of selected genes in colonic epithelial scrapings of individual FVB and *mdr1a*$^{-/-}$ mice at 12 or 25 weeks of age (FVB12, FVB25, MDR1a12, MDR1a25). The results of the real-time RT-PCR analysis are expressed as relative mRNA expression, using HPRT as a house-keeping gene. Most genes (**a** REG3A, **b** REG3G, **d** H2-DMB1, **e** CYP4B1, **f** SULT1C1, **g** NCF4) were differentially expressed between FVB and *mdr1a*$^{-/-}$ mice with a P value < 0.05, except **c** IGFBP7, $P = 0.129$). The *horizontal line* indicates the average gene expression within each sampling group

known to downregulate the activity and expression of drug-metabolizing enzymes and transporters although regulation of the phase I and phase II enzymes and transporters in inflammation is very complex [1].

In summary, our study provides further evidence of similarity in both the nature and location of intestinal inflammation in *mdr1a*$^{-/-}$ mice with that of human IBD, in particular CD. In addition, similar gene expression changes of pro-inflammatory genes and detoxification enzymes in inflamed *mdr1a*$^{-/-}$ mice compared to human IBD supports the use of this in vivo model to study IBD. Using DNA microarrays and RT-PCR we were also able to gain more insight into the nature of the epithelial response during inflammation initiation in *mdr1a*$^{-/-}$ mice. We found a

down-regulation of the anti-inflammatory REG (PAP) genes in colonic epithelial cell scrapings of 12 week old non-inflamed *mdr1a*$^{-/-}$ mice which suggest that an insufficiently suppressed immune response could be crucial to the initiation and development of intestinal inflammation in *mdr1a*$^{-/-}$ mice. Our study contributes to the development of the *mdr1a*$^{-/-}$ mice model for use in nutrigenomics experiments to investigate the anti-inflammatory potential of food components for the prevention or amelioration of inflammatory lesions and related gene expression changes in *mdr1a*$^{-/-}$ mice.

Acknowledgments Many thanks to Janice Rhodes and Hannah Smith (Crop and Food Research) for assistance with the mouse trial and Ric Broadhurst, Jason Peters, Bruce Sinclair and Kate Broadley (AgResearch Limited) for technical support throughout the study. The authors would also like to thank Julian Heyes and Juliet Sutherland (Crop and Food Research) for the valuable discussions and Katia Nones (Crop and Food Research) for proof-reading and editing the manuscript. This study is part of Nutrigenomics New Zealand, a collaboration between AgResearch, Crop & Food Research, Hort-Research and The University of Auckland that is largely funded by the Foundation for Research, Science and Technology. Matthew Barnett is funded by a Foundation for Research, Science and Technology Postdoctoral Fellowship.

References

1. Aitken AE, Richardson TA, Morgan ET (2006) Regulation of drug-metabolizing enzymes and transporters in inflammation. Annu Rev Pharmacol Toxicol 46:123–149
2. Banner KH, Cattaneo C, Le Net JL, Popovic A, Collins D, Gale JD (2004) Macroscopic, microscopic and biochemical characterisation of spontaneous colitis in a transgenic mouse, deficient in the multiple drug resistance 1a gene. Br J Pharmacol 143:590–598
3. Bilsborough J, Viney JL (2004) Out, out darn toxin: the role of MDR in intestinal homeostasis. Gastroenterology 127:339–340
4. Brant SR, Panhuysen CI, Nicolae D, Reddy DM, Bonen DK, Karaliukas R, Zhang L, Swanson E, Datta LW, Moran T, Ravenhill G, Duerr RH, Achkar JP, Karban AS, Cho JH (2003) MDR1 Ala893 polymorphism is associated with inflammatory bowel disease. Am J Hum Genet 73:1282–1292
5. Cummings JH, Antoine JM, Azpiroz F, Bourdet-Sicard R, Brandtzaeg P, Calder PC, Gibson GR, Guarner F, Isolauri E, Pannemans D, Shortt C, Tuijtelaars S, Watzl B (2004) PASSCLAIM—gut health and immunity. Eur J Nutr 43(Suppl 2):II118–II173
6. Dieckgraefe BK, Stenson WF, Korzenik JR, Swanson PE, Harrington CA (2000) Analysis of mucosal gene expression in inflammatory bowel disease by parallel oligonucleotide arrays. Physiol Genom 4:1–11
7. Folch-Puy E, Granell S, Dagorn JC, Iovanna JL, Closa D (2006) Pancreatitis-associated protein I suppresses NF-kappa B activation through a JAK/STAT-mediated mechanism in epithelial cells. J Immunol 176:3774–3779
8. Gaya DR, Russell RK, Nimmo ER, Satsangi J (2006) New genes in inflammatory bowel disease: lessons for complex diseases? Lancet 367:1271–1284
9. Grisham MB, Benoit JN, Granger DN (1990) Assessment of leukocyte involvement during ischemia and reperfusion of intestine. Methods Enzymol 186:729–742
10. Haller D (2006) Intestinal epithelial cell signalling and host-derived negative regulators under chronic inflammation: to be or not to be activated determines the balance towards commensal bacteria. Neurogastroenterol Motil 18:184–199
11. Ho GT, Moodie FM, Satsangi J (2003) Multidrug resistance 1 gene (P-glycoprotein 170): an important determinant in gastrointestinal disease? Gut 52:759–766
12. Ho GT, Soranzo N, Nimmo ER, Tenesa A, Goldstein DB, Satsangi J (2006) ABCB1/MDR1 gene determines susceptibility and phenotype in ulcerative colitis: discrimination of critical variants using a gene-wide haplotype tagging approach. Hum Mol Genet 15:797–805
13. Jessop DS, Douthwaite DA, Conde GL, Lightman SL, Dayan SM, Harbuz MS (1997) Effects of acute stress or centrally injected interleukin-1beta on neuropeptide expression in the immune system. Stress 2:133–144
14. Keilbaugh SA, Shin ME, Banchereau RF, McVay LD, Boyko N, Artis D, Cebra JJ, Wu GD (2005) Activation of RegIIIbeta/gamma and interferon gamma expression in the intestinal tract of SCID mice: an innate response to bacterial colonisation of the gut. Gut 54:623–629
15. Kuribayashi F, Nunoi H, Wakamatsu K, Tsunawaki S, Sato K, Ito T, Sumimoto H (2002) The adaptor protein p40(phox) as a positive regulator of the superoxide-producing phagocyte oxidase. EMBO J 21:6312–6320
16. Langmann T, Moehle C, Mauerer R, Scharl M, Liebisch G, Zahn A, Stremmel W, Schmitz G (2004) Loss of detoxification in inflammatory bowel disease: dysregulation of pregnane X receptor target genes. Gastroenterology 127:26–40
17. Lawrance IC, Fiocchi C, Chakravarti S (2001) Ulcerative colitis and Crohn's disease: distinctive gene expression profiles and novel susceptibility candidate genes. Hum Mol Genet 10:445–456
18. Maggio-Price L, Shows D, Waggie K, Burich A, Zeng W, Escobar S, Morrissey P, Viney JL (2002) *Helicobacter bilis* infection accelerates and *H. hepaticus* infection delays the development of colitis in multiple drug resistance-deficient (mdr1a–/–) mice. Am J Pathol 160:739–751
19. Mathew CG, Lewis CM (2004) Genetics of inflammatory bowel disease: progress and prospects. Hum Mol Genet 13(Spec No 1):R161–R168
20. Panwala CM, Jones JC, Viney JL (1998) A novel model of inflammatory bowel disease: mice deficient for the multiple drug resistance gene, mdr1a, spontaneously develop colitis. J Immunol 161:5733–5744
21. Podolsky DK (2002) The current future understanding of inflammatory bowel disease. Best Pract Res Clin Gastroenterol 16:933–943
22. Puleston J, Cooper M, Murch S, Bid K, Makh S, Ashwood P, Bingham AH, Green H, Moss P, Dhillon A, Morris R, Strobel S, Gelinas R, Pounder RE, Platt A (2005) A distinct subset of chemokines dominates the mucosal chemokine response in inflammatory bowel disease. Aliment Pharmacol Ther 21:109–120
23. Reeves PG, Nielsen FH, Fahey GC Jr (1993) AIN-93 purified diets for laboratory rodents: final report of the American Institute of Nutrition ad hoc writing committee on the reformulation of the AIN-76A rodent diet. J Nutr 123:1939–1951
24. Schinkel AH, Smit JJ, van Tellingen O, Beijnen JH, Wagenaar E, van Deemter L, Mol CA, van der Valk MA, Robanus-Maandag EC, te Riele HP (1994) Disruption of the mouse mdr1a P-glycoprotein gene leads to a deficiency in the blood–brain barrier and to increased sensitivity to drugs. Cell 77:491–502
25. Schwab M, Schaeffeler E, Marx C, Fromm MF, Kaskas B, Metzler J, Stange E, Herfarth H, Schoelmerich J, Gregor M,

Walker S, Cascorbi I, Roots I, Brinkmann U, Zanger UM, Eichelbaum M (2003) Association between the C3435T MDR1 gene polymorphism and susceptibility for ulcerative colitis. Gastroenterology 124:26–33

26. Tak PP, Firestein GS (2001) NF-kappaB: a key role in inflammatory diseases. J Clin Invest 107:7–11
27. Yantiss RK, Odze RD (2006) Diagnostic difficulties in inflammatory bowel disease pathology. Histopathology 48:116–132